Coarsening of bicontinuous structures via nonconserved and conserved dynamics

Yongwoo Kwon,[1] Katsuyo Thornton,[2] and Peter W. Voorhees[1,*]
[1]*Department of Materials Science and Engineering, Northwestern University, 2220 Campus Drive, Evanston, Illinois 60208-3108, USA*
[2]*Department of Materials Science and Engineering, 2300 Hayward Street, University of Michigan, Ann Arbor, Michigan 48109-2136, USA*

(Received 27 October 2006; published 26 February 2007)

Coarsening subsequent to phase separations occurs in many two-phase mixtures. While unique scaled particle size distributions have been determined for highly asymmetric mixtures in which spherical particles form in a matrix, it is not known if a unique scaled structure exists for symmetric mixtures, which yield bicontinuous structures having intricately interpenetrating phase domains. Using large-scale simulations, we have established that unique scaled microstructures exist in symmetric mixtures evolving via nonconserved and conserved dynamics. We characterize their morphologies by the interfacial shape distribution, a counterpart to the particle size distribution, and their topologies by the genus. We find that the two dynamics result in unique, but different, scaled interfacial shape distributions, with conserved dynamics yielding a narrower distribution around zero mean curvature. In contrast, the two scaled structures are topologically similar, having nearly equal values of the scaled genus.

DOI: 10.1103/PhysRevE.75.021120 PACS number(s): 64.60.−i, 64.70.−p, 64.75.+g, 81.30.−t

Phase separation occurs in a vast array of systems, from ferromagnetic materials to polymers, in which a homogeneous single phase separates into two phases when cooled below the critical temperature. When the concentrations in the two phases are at nearly their equilibrium values, a coarsening process ensues. This process is driven by the excess free energy associated with the presence of interfaces between phases. This energy can be reduced by decreasing the total interfacial area of the system, which results in the coarsening of structures. It has been established that in certain cases the coarsening process is self-organizing such that the interfacial morphology becomes self-similar, i.e., time independent when scaled by a time-dependent characteristic length of the system, after a sufficient coarsening time. This self-organizing behavior has been investigated extensively for systems that are composed of a polydisperse array of particles embedded in a matrix. In this case, Lifshitz and Slyozov [1], and Wagner [2] (LSW) predicted that the particle size distribution will attain a unique time-independent shape when scaled by the average particle radius $\bar{R}$.

However, there is a large array of phase separation processes that do not yield such particles in a matrix, but instead result in *bicontinuous* structures, where phases are interpenetrating and intricately connected. Such bicontinuous structures frequently arise in spin ordering in magnetic materials [3,4], spinodal decomposition in binary homopolymer mixtures [5–7], order-disorder transformation [8,9], phase separation [10,11], and in microemulsions [12]. It has been known that the morphologies of bicontinuous structures found in block copolymers are related to those of periodic surfaces with zero mean curvature, so-called minimal surfaces [13–16]. In contrast, in the case of surface-tension driven dynamics minimal surfaces are unstable to small morphological perturbations [17], and thus cannot result from a coarsening process.

The interfacial morphologies of three-dimensional bicontinuous interfaces that are present during coarsening is a matter of great controversy. In most cases the interfacial morphology has been characterized with indirect measures of the interfacial structure, such as the two-point spatial correlation function, or its Fourier transform, the structure function. While it is well known that the structure function scaled by a characteristic length l, corresponding to $\bar{R}$ of the particle coarsening case, becomes self-similar during coarsening [18–21], it is unclear if the interfacial morphologies attain self-similarity or how they may differ from that of minimal surfaces. For example, in the simulations by Aksimentiev [22], where the interfacial strucuture was characterized for conserved-order-parameter coarsening, self similarity was not observed, and while Fiałkowski *et al.* did observe scaling of the interfacial curvature for nonconserved-order-parameter coarsening [23], Brown and Rikvold claim that these are transient states [24]. Thus it is necessary to characterize quantitatively the morphology of these two-phase mixtures in the very late stages of the transformation process where scaling may exist. If these structures could be characterized accurately and if the measures used to quantify the morphologies exhibit scaling, then the counterpart for these bicontinuous structures to the well-known scaled particle-size distribution found many years ago by LSW would finally be known. Furthermore, if such unique structures exist, one could determine whether the interfacial morphologies and their evolution depend on the mechanism of coarsening. These unique structures would also form the basis of comparison for future work on systems in which other effects such as anisotropic interfacial energy, external fields, hydrodynamic flows, and asymmetric volume fractions play a role in the interfacial evolution during coarsening.

We shall examine coarsening following phase separation by *nonconserved* and *conserved* dynamics (model A and model B, respectively) using a technique for characterizing the morphologies of highly complex structures [16,22,25,26]. The bicontinuous structures are obtained by numerically solving the Allen-Cahn (AC) equation [8] and

*Electronic address: p-voorhees@northwestern.edu

the Cahn-Hilliard (CH) equation [27] for the systems with nonconserved and conserved dynamics, respectively. The AC equation is also called the time-dependent Ginzburg-Landau equation. We examine both conserved and nonconserved dynamics because coarsening proceeds via different mechanisms in these two cases. Coarsening via conserved dynamics takes place by long-range diffusion of mass and thus describes the evolution of a conserved order parameter such as the concentration. The initial phase separation process in this case is called spinodal decomposition. On the other hand, nonconserved dynamics does not require long-range diffusion of mass and thus describes the evolution of a nonconserved order parameter such as magnetization or compositional order. The initial phase separation in this case is called phase ordering. In both dynamics, the motion of the interface is related to its mean curvature. In coarsening with conserved dynamics, the diffusion field at a point is determined by the mean curvature of the surrounding interfaces. Therefore the factors influencing the interfacial velocity at that point are *nonlocal*. In contrast, the velocity of the interface depends only upon its *local* mean curvature in the nonconserved dynamics case.

We choose as simple a model as possible. We examine only critical quenches that yield equal volume fractions of two phases in a symmetric phase diagram. The evolution of the order parameter for a two-phase system with isotropic interfacial energy is described by the following dimensionless equation:

$$\frac{\partial \phi}{\partial t} = -(-\nabla^2)^p \left[\frac{df}{d\phi} - \nabla^2 \phi \right], \tag{1}$$

where ϕ is the order parameter, t is dimensionless time, and f is the dimensionless free energy density given by $(1/4)\phi^2(1-\phi)^2$. For $p=0$ we obtain the AC equation and nonconserved dynamics, whereas for $p=1$ we obtain the CH equation and conserved dynamics. The double well free energy has a well height of $1/64$ at $\phi=1/2$ and minima at the two equilibrium values of the order parameter ($\phi=0,1$), each representing a phase. The order parameter varies continuously from one value to another across an interface and thus yields a finite interfacial thickness; that is, the interface is diffuse [28]. A flat interface located at $x=0$ in equilibrium will yield an order parameter profile, $\phi(x)=(1/2)[1-\tanh(x/2\sqrt{2})]$. In this simple model, the chemical potential, the term in the square brackets in Eq. (1), is the same for both dynamics and thus the only difference between them is whether the order parameter is conserved. These equations are solved using periodic boundary conditions and a finite-difference algorithm with spatially centered, temporally forward-Euler scheme implemented on a multiple processor parallel computing platform. Data are only collected in the late stages of the coarsening, when the interfacial thickness is at its equilibrium value and the principal radii of curvatures are much larger than the interfacial thickness. This, along with the need to avoid finite size effects, necessitates that large system sizes be employed with an interface as thin as possible [29]. We thus use 512^3 and 1024^3 computational grids for the conserved and nonconserved dynamics, respectively, with a grid spacing of $2\sqrt{2}$ which provides three grid points in the interfacial region where $0.1 \leqslant \phi \leqslant 0.9$. While the number of mesh points is lower than those employed in a typical phase-field calculations, we have verified that this resolution is sufficient by comparing simulations with this and higher resolutions. We found no significant differences between the results obtained in the two cases.

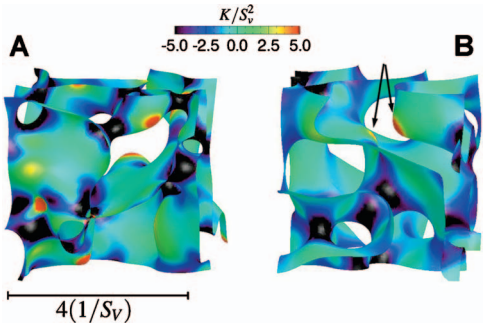

FIG. 1. (Color) A small portion of the computational domain with interfaces colored with the scaled Gaussian curvature, K/S_V^2. A: Interfacial morphology in a system with a nonconserved order parameter (model A), $t=1600$ $(1/S_V=101.40)$; B: interfacial morphology in a system with a conserved order parameter (model B), $t=588\,800$ $(1/S_V=71.96)$. Both portions are cubic domains with edge lengths of $4(1/S_V)$. In B, the pair of red regions marked with arrows is a remnant of a pinched tube. More red regions are observed in the interfacial structure evolving by nonconserved dynamics.

Figure 1 shows the bicontinuous structures resulting from our simulations. Although both interfacial structures are bicontinuous, their morphologies are different, as evident by the presence of red regions of strongly positive Gaussian curvature (interfaces with large curvatures that are concave or convex but not saddle-shaped) in systems with a nonconserved order parameter.

The kinetics of the late-stage coarsening process is described by temporal power laws for a characteristic length, $l \sim t^n$, where n is $1/2$ and $1/3$ for nonconserved and conserved dynamics, respectively. We use $1/S_V$ for l, where S_V is the surface area per volume. While these power laws hold if the coarsening process is self-similar, the converse is not true. That is, it is possible that the evolution is not self-similar even if $1/S_V \sim t^n$ [30,31]. We find the growth exponents for simulated nonconserved and conserved dynamics to be $n=0.491$ and 0.327 with standard errors of 0.003 and 0.001, respectively. These numbers are close to the theoretical values.

We calculate the mean curvature (H) and Gaussian curvature (K) of the interfaces. We then construct the interfacial shape distribution (ISD), $P(\kappa_1,\kappa_2)$, which is defined as the probability of finding a patch of interface with a certain pair of minimum and maximum principal curvatures. The principal curvatures κ_1 and κ_2 are determined using the calculated H, K and the definitions: $H=(\kappa_1+\kappa_2)/2$ and $K=\kappa_1\kappa_2$. The ISD is the counterpart for arbitrarily curved surfaces to the particle size distribution for systems with spherical particles. If both κ_1 and κ_2 have the same sign, the interfacial patch is parabolic or elliptic. If κ_1 is negative and κ_2 is positive, the

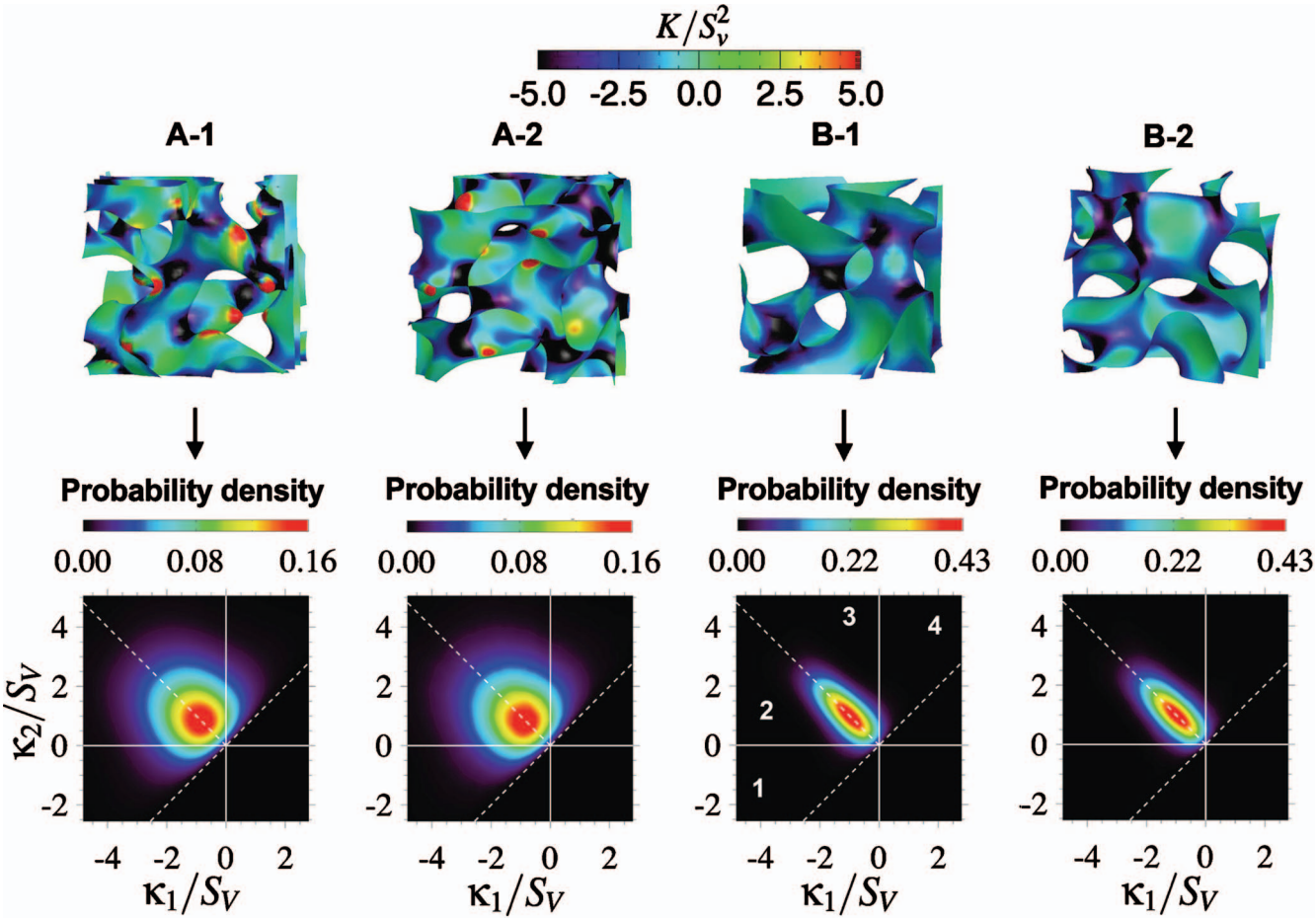

FIG. 2. (Color) Portions of the interfaces colored with K/S_V^2, such that the edge length of each cube is $4(1/S_V)$, and ISDs scaled by S_V obtained from the whole simulated structures. A-1: Nonconserved order parameter, $t=480$ $(1/S_V=56.79)$; A-2: nonconserved order parameter, $t=4\,000$ $(1/S_V=158.93)$; B-1: conserved order parameter, $t=64\,000$ $(1/S_V=35.61)$; B-2: Conserved order parameter, $t=179\,200$ $(1/S_V=77.81)$. There are four possible regions in the ISDs, divided by lines where $\kappa_1=\kappa_2$ on which spherical patches lie, $\kappa_1=-\kappa_2$ on which patches with zero mean curvature $(H=0)$ lie, and $\kappa_i=0$ $(i=1,2$; two axis lines) on which cylindrical patches with zero Gaussian curvature lie. The planar patches $(\kappa_1, \kappa_2=0)$ lie at the origin. All physically attainable surfaces lie to the left of the $\kappa_1=\kappa_2$ line since by our definition $\kappa_2 \geqslant \kappa_1$. Regions 1 and 4 contain patches with positive Gaussian curvature (parabolic or elliptic patches) while regions 2 and 3 contain patches with negative Gaussian curvature (hyperbolic or saddle-shaped patches). Note that the color bars of ISDs in A-1 and A-2 are different from those in B-1 and B-2.

patch is hyperbolic or saddle-shaped. Figure 2 shows that the scaled ISDs evolving by nonconserved dynamics (A-1 and A-2) and conserved dynamics (B-1 and B-2) are independent of time. The coarsening process is accompanied by decreasing curvatures and increasing $1/S_V$. Without scaling by S_V, the ISDs become smaller and their peaks move toward the origin. *The invariance of the scaled ISDs with time indicates that the morphologies produced by nonconserved and conserved dynamics are self-similar in the late-stage coarsening.*

More importantly, however, the shapes of the scaled ISDs of two dynamics are clearly different. Consistent with equal volume fractions of the two phases, both of the scaled ISDs are symmetric about the $H=0$ $(\kappa_1=-\kappa_2)$ line and the average of H over the structure is zero. The majority of the interfaces are hyperbolic, also termed saddle-shaped. The peaks of both ISDs are near $-\kappa_1 S_V^{-1} \approx \kappa_2 S_V^{-21} \approx 1$, implying that S_V provides a good order-of-magnitude measure of the interfacial curvature.

The scaled ISD for nonconserved dynamics has a larger deviation from the $H=0$ line than that of the conserved dynamics. The standard deviations in scaled mean curvature $(\sqrt{\langle H^2 \rangle}/S_V)$ are 0.94 and 0.34 for nonconserved and conserved dynamics, respectively. The interfacial velocity for nonconserved dynamics is *local* and is solely a function of the mean curvature at a point. By contrast, the interfacial velocity for conserved dynamics is *nonlocal*, governed by the diffusion field established by mean curvatures of surrounding patches. Therefore the interfacial velocity of an interfacial patch is more strongly coupled with those of surrounding patches in conserved dynamics than in nonconserved dynamics. The coupling results in rapid evolution of an interfacial patch toward reducing the local curvature variation and thus increases the stablility of regions with similar curvatures. This nonlocal coupling only exists in conserved dynamics, which leads to the observed smaller deviation in the mean curvature and narrower ISDs. Also evident is the larger fraction of interface with $K>0$ in the

scaled ISD for nonconserved dynamics than for conserved dynamics, as seen in the interfacial structures of Figs. 1 and 2. There are more red regions in structures evolving by nonconserved dynamics. Those red regions have strongly positive K, mostly appear as pairs separated by a relatively small distance, and thus are likely remnants of a thin tube-shaped region of a phase that fissioned into two parts.

By integrating the scaled ISDs over regions 1 and 4, we find that ~20% and ~6% of the interfacial area have $K>0$ during coarsening by nonconserved and conserved dynamics, respectively. Unlike H, the average of K is nonzero in agreement with results presented by Aksimentiev, Moorthi, and Hołyst [22]. However, Aksimentiev *et al.* did not find the self-similar evolution in their simulations. The scaled ISDs shown in Fig. 2 are unique to the corresponding dynamics during the self-similar evolution of bicontinuous structures, and thus are the counterparts to the well known LSW particle-size distribution for a system with spherical particles.

Pinching of tubes is a topologically singular event, and thus it changes the topology of the bicontinuous structures. We use the genus (g), defined as the number of cuts that can be made upon a closed surface without separating it into two disconnected bodies, to quantify the topology of the bicontinuous structures. By this definition, a cube, sphere, and pyramid are all topologically equivalent ($g=0$) while a cube with a handle and a doughnut are equivalent ($g=1$). Pinching of tubes decreases the genus while merging of separated parts increases the genus. Since the phases are completely interconnected, the genus per volume, g_V, can thus be interpreted as the number density of tunnels or tubes in the system. Therefore the larger g_V the more topologically complicated is its structure. During coarsening of bicontinuous structures, g_V decreases due to the pinching which is needed for the self-similar growth of bicontinuous networks. We calculate g using the Gauss-Bonnet (GB) theorem, $g=1-(4\pi)^{-1}\int_S KdS$, where S denotes the interface, to investigate the evolution of g_V.

We find that the genus per unit volume changes with time as $g_V \sim t^{n_g}$ where $n_g=-1.48$ and $n_g=-1.00$ with the standard errors of 0.03 and 0.08 for coarsening in systems with nonconserved and conserved order parameters, respectively. Since g_V is proportional to $1/V$, these exponents agree with those obtained from the power law for inverse characteristic volume, $(1/S_V)^3 \sim (t^n)^3$. This implies that $g_V S_V^{-3} \sim t^{n_g+3n}$, where n_g+3n is 0 for both dynamics, and thus $g_V S_V^{-3}$ is time independent. We define this dimensionless number, $g_V S_V^{-3}$, as the scaled genus, representing the genus per characteristic volume. The simulation indeed shows that the scaled genus is invariant in time, as shown in Fig. 3. It is remarkable that the values of the scaled genus for both dynamics are similar, implying nearly identical numbers of tunnels per unit characteristic volume based on the cube of the surface area per unit volume.

For structures where $g \gg 1$, the GB theorem becomes $g \simeq -(4\pi)^{-1}\int_S KdS$. Multiplying both sides by $V^{-1}S_V^{-3}$, we obtain $g_V S_V^{-3} \simeq -(4\pi)^{-1} K_{avg} S_V^{-2}$, where $K_{avg}=(VS_V)^{-1}\int_S KdS$. Just like the scaled genus, the scaled average Gaussian curvatures ($K_{avg}S_V^{-2}$) is time-invariant and similar in both dynamics during coarsening. Thus the scaling of morphologies or ISDs automatically implies the scaling of the topologies. This similar scaled topology with different scaled morphologies is due to the fact that the conserved and nonconserved dynamics result in similar values in $K_{avg}S_V^{-2}$.

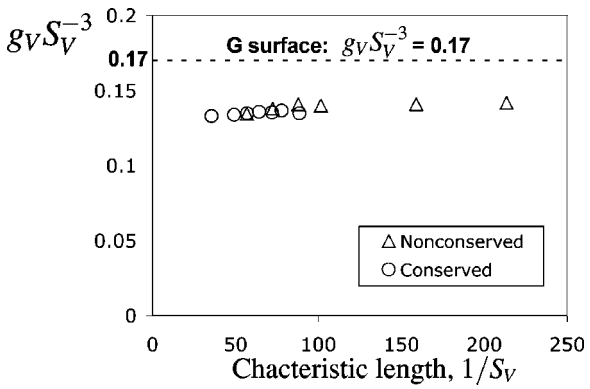

FIG. 3. Genus per characteristic volume ($g_V S_V^{-3}$) vs characteristic length ($1/S_V$).

We compare the bicontinuous structures from our simulations with Schoen's G surface, one of triply periodic minimal surfaces, having a genus per unit cell of 5. This minimal surface has been used as a model for the interfacial structure of the bicontinuous structures in many block copolymer systems [14–16]. We demonstrate how the bicontinuous structures from phase separation are topologically and morphologically different from the G surface by means of the scaled genus and the ISD. We determine the scaled genus of the G surface with volume fraction of 50:50 and S_V of 0.31, based on the data given by Góźdź *et al.* [32] and obtain the scaled genus of 0.17 for the G surface, which is 21% larger than 0.14 found for the self-similar structures resulting from phase separation. While the difference is modest, it is statistically significant since it is much larger than any fluctuation in the scaled genus obtained in the simulations, indicating that the topology of the self-similar structures differs from that of the G surface. The difference in the ISD is more dramatic. The approximate minimum value of scaled Gaussian curvature $[K/S_V^2=(\kappa_1/S_V)(\kappa_2/S_V)]$ is −1.83 for the G surface (obtained from the histrogram given by Góźdź *et al.*) that is much less than −7.84 for structures with conserved dynamics (obtained from the ISDs in Fig. 2). The absolute values of standard deviation of the scaled mean curvature of the G surface is zero by definition while the standard deviations in H/S_V of the self-similar structures given earlier are clearly nonzero. The scaled genus, the Gaussian curvature, and the mean curvature all point to the fact that the self-similar bicontinuous structures originated from phase separation and coarsening are quantitatively different not only in their morphology but also their topology from a minimal surface, regardless of the mechanism of coarsening.

We investigated the evolution of the interfacial morphology and topology during coarsening via nonconserved and conserved dynamics subsequent to phase separation. In both dynamics, we find self-similar evolution of topological and morphological characteristics, the genus and the interfacial

shape distribution, respectively. This result indicates that the interfacial morphologies that undergo coarsening following phase separation with equal phase fractions are described by the interfacial shape distributions given above. However, the interfacial shape distributions of the self-similar structures of the two dynamics are different, with conserved dynamics yielding narrower distribution of interfacial curvature about zero mean curvature. The difference is attributed to the stronger coupling of interfacial curvatures in the conserved dynamics case. In contrast, the two scaled structures are topologically similar, as evident from the similar values of the scaled genus; thus the connectivities of the two bicontinuous structures are similar. We also showed that the morphology and topology of the bicontinuous structures originated from phase separation differ from that of the well-known Schoen's *G* surface.

This work was supported by the National Aeronautics and Space Administration, and the Office of Naval Research and DARPA as part of the Dynamic 3-D Digital Structure Program. K.T. acknowledges the financial support from DOE under Grand No. DE-FG02–05ER46191.

[1] I. M. Lifshitz and V. V. Slyozov, J. Phys. Chem. Solids **19**, 35 (1961).
[2] C. Wagner, Z. Elektrochem. **65**, 581 (1961).
[3] M. Fiałkowski and R. Hołyst, Phys. Rev. E **66**, 046121 (2002).
[4] O. Hellwig, A. Berger, and E. E. Fullerton, Phys. Rev. Lett. **91**, 197203 (2003).
[5] M. Lorén, M. Langton, and A.-M. Hermansson, J. Chem. Phys. **116**, 10536 (2002).
[6] H. Jinnai, H. Watashiba, T. Kajihara, and M. Takahashi, J. Chem. Phys. **119**, 7554 (2003).
[7] E. Scholten, L. M. C. Sagis, and E. van der Linden, Macromolecules **38**, 3515 (2005).
[8] S. M. Allen and J. W. Cahn, Acta Metall. **27**, 1085 (1979).
[9] M. Carpenter, Science **206**, 681 (1979).
[10] K. Stratford *et al.*, Science **309**, 2198 (2005).
[11] Y. Iwashita and H. Tanaka, Nat. Mater. **5**, 147 (2006).
[12] M. Clausse *et al.*, Nature (London) **293**, 636 (1981).
[13] L. E. Scriven, Nature (London) **263**, 123 (1976).
[14] E. L. Thomas, D. M. Anderson, C. S. Henkee, and D. Hoffman, Nature (London) **334**, 598 (1988).
[15] D. A. Hajduk *et al.*, Macromolecules **27**, 4063 (1995).
[16] H. Jinnai, Y. Nishikawa, R. J. Spontak, S. D. Smith, D. A. Agard, and T. Hashimoto, Phys. Rev. Lett. **84**, 518 (2000).
[17] B. Davidovitch, D. Ertaş, and T. C. Halsey, Phys. Rev. E **70**, 031609 (2004).
[18] Y. C. Chou and W. I. Goldburg, Phys. Rev. A **23**, 858 (1981).
[19] M. Hennion, D. Ronzaud, and P. Guyot, Acta Metall. **30**, 599 (1982).
[20] H. Furukawa, Physica A **123**, 497 (1984).
[21] T. Hashimoto, M. Itakura, and H. Hasegawa, J. Chem. Phys. **85**, 6118 (1986).
[22] A. Aksimentiev, K. Moorthi, and R. Holyst, J. Chem. Phys. **112**, 6049 (2000).
[23] M. Fiałkowski, A. Aksimentiev, and R. Hołyst, Phys. Rev. Lett. **86**, 240 (2002).
[24] G. Brown and P. A. Rikvold, Phys. Rev. E **65**, 036137 (2002).
[25] J. Alkemper and P. W. Voorhees, Acta Mater. **49**, 897 (2001).
[26] R. Mendoza, I. Savin, K. Thornton, and P. W. Voorhees, Nat. Mater. **3**, 385 (2004).
[27] J. W. Cahn, Acta Metall. **9**, 795 (1961).
[28] J. W. Cahn and J. E. Hilliard, J. Chem. Phys. **28**, 258 (1958).
[29] R. Toral, A. Chakrabarti, and J. D. Gunton, Phys. Rev. Lett. **60**, 2311 (1988).
[30] R. Mendoza, J. Alkemper, and P. W. Voorhees, Z. Metallkd. **96**, 155 (2005).
[31] D. Kammer and P. W. Voorhees, Acta Mater. **54**, 1549 (2006).
[32] W. T. Góźdź and R. Hołyst, Phys. Rev. E **54**, 5012 (1996).